Automatic Internal Segmentation of Caudate Nucleus for Diagnosis of Attention Deficit Hyperactivity Disorder

Laura Igual⋆, Joan Carles Soliva†, Roger Gimeno⋆, Sergio Escalera⋆, Oscar Vilarroya†, and Petia Radeva⋆

⋆ Department of Applied Mathematics and Analysis, Universitat of Barcelona, and Computer Vision Center of Barcelona, Spain
† Unitat de Recerca en Neurociència Cognitiva, Department of Psychiatry, and Universitat Autònoma de Barcelona and Fundació IMIM, Spain

Abstract. Studies on volumetric brain Magnetic Resonance Imaging (MRI) showed neuroanatomical abnormalities in pediatric Attention Deficit Hyperactivity Disorder (ADHD). In particular, the diminished right caudate volume is one of the most replicated findings among ADHD samples in morphometric MRI studies. In this paper, we propose a fully-automatic method for internal caudate nucleus segmentation based on machine learning. Moreover, the ratio between right caudate body volume and the bilateral caudate body volume is applied in a ADHD diagnostic test. We separately validate the automatic internal segmentation of caudate in head and body structures and the diagnostic test using real data from ADHD and control subjects. As a result, we show accurate internal caudate segmentation and similar performance among the proposed automatic diagnostic test and the manual annotation.

Keywords: Automatic Caudate Segmentation, Attention Deficit Hyperactivity Disorder, ADHD Diagnosis.

1 Introduction

Attention Deficit Hyperactivity Disorder (ADHD) is a developmental disorder characterized by inattentiveness, motor hyperactivity and impulsiveness, which represents the most prevalent psychiatric disorder in childhood. Moreover, it is estimated that half of children with ADHD will display the disorder in adulthood. Studies on volumetric brain Magnetic Resonance Imaging (MRI) show neuroanatomical abnormalities in pediatric ADHD [1]. As stated in several reviews and metanalyses, the diminished right caudate volume is one of the most replicated findings among ADHD samples in morphometric MRI studies [7, 3, 10]. As a result, in [8] the authors proposed a diagnostic test based on volumetric measures of caudate nucleus regions.

Most of the studies for ADHD analysis in MRI images, as well as many research works in neuroscience, lack of an appropriate segmentation system, and

thus, require experts to manually segment brain structures, as the caudate nucleus, on a slice by slice basis. For caudate segmentation, as well as the external delineation of the boundary, it is necessary to internally segment the head and body areas. This process is extremely time consuming, tedious, and prone to inter-rater discrepancies, limiting the statistical power of the presented analysis. Automatic external segmentation of subcortical structures in the brain is a difficult problem, but acceptable solutions can be found. In [10], a manual strategy for internal caudate segmentation was proposed based on a simple geometric criterion. However, up to our knowledge, there is not any method in the literature for automatic internal segmentation of caudate nucleus. Strategies towards mental diseases understanding and diagnosis are based on useful shape descriptors, as is done in [2] or [4], where a shape descriptor is used for thalamus classification. However, caudate nucleus is a small structure and these descriptors have troubles in caudate representation and discrimination. In this work, we propose a new automatic internal segmentation to separate caudate head and body parts learning a classifier based on shape features of the Region of Interest (ROI). Moreover, we define an automatic diagnostic test based on the ratio between right caudate body volume (rCBV) and the bilateral caudate body volume (bCBV), following the manual test proposed in [8]. The results on real data ADHD and control subjects are similar between the fully-automatic obtained results and the manual ones provided in [8].

The rest of the paper is organized as follows: Section 2 presents the method for automatic external and internal caudate segmentation and ADHD diagnosis. Section 3 shows the experimental results, and Section 4 concludes the paper.

2   Method

The proposed method is split in three main steps: 1) external caudate segmentation, 2) internal caudate segmentation: head and body separation, and 3) diagnostic test. Figure 1 shows the method pipeline. Step 1) is performed using the recently proposed CaudateCut segmentation algorithm [5] especially conceived for the caudate boundary delineating in MRI slices and based on the Graph Cut (GC) framework [6]. Steps 2) and 3) are described next.

2.1   Internal segmentation: head and body separation

Given the external segmentation of the caudate nuclei in the MRI slices, we identify the images corresponding to caudate head from the caudate body ones. Prior information of caudate shape in axial view of MRI volumes asserts that caudate head structure tends to be wider, while the body one tends to be elongate [10]. Moreover, first caudate slices in the axial projection of the MRI correspond to the head and the last ones to the body. An example of head and body caudate regions are shown in Figure 2 (a-b).

We propose two different strategies to perform the internal segmentation based in internal shape and avoiding the use of caudate neighbor structures as
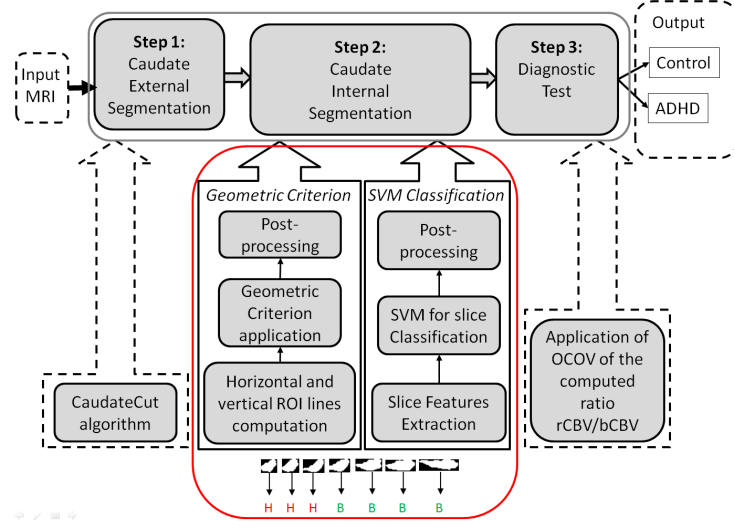
Fig. 1. Overview of the diagnostic test pipeline.

references. First, we propose an automatic algorithm of the manual geometric criterion analysis proposed in [10] using Computer Vision techniques. Second, we use Support Vector Machines (SVM) to train a classifier able to recognize head and body ROIs. Finally we apply a postprocessing step based on Decision Stump to filter the slice classification and improve final prediction.

Automatic Geometric Criterion classification. Authors in [10] define a geometric criteria according to which head and body ROIs have to verify: $h \leq 2w(Head), h > 2w(Body)$, where h and w are the height and width of the ROI, respectively. The underlying idea of this geometric criteria is relatively intuitive and its automation is simple. First, the MRI volumes must be oriented in the AC-PC line [9]. The MRI caudate slices with ROI whose bounding box area is lower than 50 pixels are discarded in order to avoid noisy regions. Then, the two larger horizontal and vertical lines within the ROI are computed (Figure 2 (c-d)). Finally, the geometric criterion is applied using the length of these lines (in pixels) and the image is classified as head or body.

Shape-based SVM classification. In order to improve caudate head and body separation, we propose an alternative method based on the extraction of an extended set of caudate region features and the classification using SVM. The set of features is composed by: ROI area, ratio between height and width of the ROI, height, width and area of the bounding box containing the ROI, extent (ratio of pixels in the ROI and pixels in the total bounding box), major and minor axis length of the ellipse that has the same normalized second central moments as the ROI, orientation of the ellipse, eccentricity (ratio of the distance between the
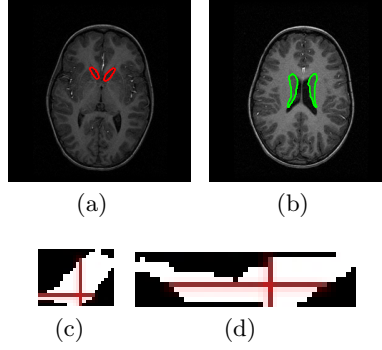
Fig. 2. Example of (a) caudate head image, and (b) caudate body image, with caudate nuclei marked in white. Examples of (c) head ROI and (d) body ROI with the two larger horizontal and vertical lines depicted in red.

foci of the ellipse and its major axis length), perimeters ratio (relation between the perimeter of the circle with the same area as the ROI, and the perimeter of the ROI), and x and y coordinates of the centroid. Once we compute the set of features of the caudate regions we use SVM classifier to classify head and body caudate regions.

Post-processing: Decision Stumps. The Decision Stump (DS) technique is a machine learning model that consists of one-level decision tree. A DS makes a polarity prediction based on the value of just a single input feature. DS is often used as a weak classifier in machine learning ensemble techniques. Here, we use DS to find a unique separation between caudate head and body areas. The procedure used is as follows, the error weight for each class is set to:

$$\omega_e(Head) = \frac{1}{\#Head\ images}, \omega_e(Body) = \frac{1}{\#Body\ images}$$

A loss function describing the importance in the order of appearance of head and body images is defined for each case. The loss function, F_x for head and body is linear and cubic, respectively, since we want to strongly penalize the apparition of body regions in the first positions. Previous analysis says that 60% to 70% of the total of caudate slices belongs to caudate head. Once the weight and loss function are defined, the system searches for the optimal division between caudate head and body sections in terms of error, computing it as $\omega_e * F_x$. The position giving the smallest error will be selected as the separation position and the images will be consequently relabeled. After applying DS, most of the cases where there are images classified as head in the middle of a body section or vice versa disappear, and the global classification is in consequence improved.

2.2 Diagnostic Test

The objective of the diagnostic test is to discriminate between MRI volumes corresponding to ADHD and healthy subjects. In [8], authors present a diagnostic test to assist in the diagnosis of ADHD in children based on the ratio rCBV/bCBV. Using the Receiver Operating Characteristic (ROC) curve analysis on the defined ratio, the Optimal Cut-Off Value (OCOV) is estimated as the optimal ratio for which the specificity is greater or equal than a threshold Th_{spec}, and can be applied to classify new subjects.

3 Results

In this section, we evaluate the performance of the three steps of the diagnostic test using ADHD and control subjects.

3.1 Data and Validation Measures

The study population includes 39 children with ADHD according to DSM-IV (referred from the Unit of Child Psychiatry at Hospital Vall Hebron in Barcelona) and 39 control subjects. Children with ADHD received a consensus diagnosis by an expert team (see [1] for a detailed explanation). For all subjects in the population MRI 1.5-T system volumes were used. MRI volumes were analyzed by its axial projection, which consists on 60 image planes with a resolution of 256 by 256 pixels. The volume of each voxel is $0.94 \times 0.94 \times 2$ mm^3.

For validation of the automatic caudate internal segmentation, we consider as ground truth the manual annotation of the data following the procedure described in [10] by means of an expert.

We computed the following three validation measures based on True Positive (TP), False Positive (FP), True Negative (TN) and False Negative (FN): Sensitivity $= \frac{TP}{TP+FN}$, Specificity $= \frac{TN}{TN+FP}$, Accuracy $= \frac{TP+TN}{TP+TN+FP+FN}$. In the internal caudate segmentation validation, head corresponds to positive and body to negative. In the diagnostic test validation: ADHD patients corresponds to positive and control subjects to negative.

3.2 Caudate Nuclei Segmentation

Internal Segmentation. In order to evaluate the proposed methods we divided in two subsets the set of 1039 caudate images from the 78 subjects, one for training and one for testing. In Table 1, we summarize the comparative between Geometric Criterion approach (GC) and Linear, Polynomial and RBF kernel SVM strategies in terms of accuracy. One of the main problems was the small range of values of the quotient h/v of the criterion. Moreover, in Table 1, it is possible to see the improvement obtained with DS. From these results, it can be inferred that the best strategy is the one using linear SVM with DS. In order to train RBF and Polynomial SVM, 3-fold cross validation was used. The good

	GC	**L-SVM**	P-SVM	RBF-SVM
without DS	87.3%	91.5%	90.8%	90.4%
with DS	87.1%	**92.8%**	91.8%	91.6%

Table 1. Accuracy of internal segmentation strategies: Geometric criteria (GC), SVM with different kernels: Linear, Polynomial and RBF kernel and without or with DS application. Best results are marked in bold.

Accuracy	Sensitivity	Specificity
92.05%	92.27%	92.50%

Sensitivity	Specificity	OCOV
48.72%	84.62%	0.4828

Table 2. Results obtained for the internal caudate segmentation (first row) and for the diagnostic test (second row). Both cases using the leave-one-out validation strategy.

	Mean	σ	Mean Diff.	t	p
Control	0.53	0.06	0.05	2.4086	0.0092
ADHD	0.48	0.05			

Table 3. Statistical analysis: mean of the ratio rCBV/bCBV and standard deviation (σ) for control and ADHD groups, difference of means of the groups, t-value of the t-test (with 0.05%), p-value and confidence interval.

performance of our method is shown in Table 2 (first row), where we show the accuracy, sensitivity and specificity of linear SVM with DS using leave-one-out validation strategy on the whole set of images.

External Segmentation. As it is reported in [5], the CaudateCut method obtained volumetric mean overlap of 82.60% on the data introduced above.

3.3   Diagnostic analysis

First, to analyze the significance of the ratio (rCBV/bCBV) in discriminating ADHD and control groups, we performed a Student's t-test (with a threshold of $p < 0.05$). Table 3 summarizes the obtained statistics. In particular, mean ratio values, their standards deviation, the difference of means between the two groups and the results of the t-test are included. The result of the t-test was positive, confirming the statistical significance of the ratio measure.

Second, in order to compare the proposed automatic strategy with the manual one we followed the validation steps indicated in [8]. In particular, we divided the set of 78 subjects in two subsets, one used for training and another for testing. We performed a ROC curve analysis using the training set to learn the OCOV as the optimal ratio threshold where the specificity was greater or equal than 85%. Table 4 shows the discriminative power of the system to differentiate between control and ADHD subjects. First row includes the results obtained in

External seg./Internal seg.	Sensitivity	Specificity	AUC	OCOV
Manual/Manual [8]	60%	95%	0.84	0.4818
Manual/Manual (replica)	55%	85%	0.73	0.483
CaudateCut / SVM Linear+DS	68.42%	89.47%	0.75	0.491

Table 4. Sensitivity, specificity, Area Under Curve (AUC), and Optimal Cut-Off Value (OCOV) on the training set for different combinations of external and internal segmentations.
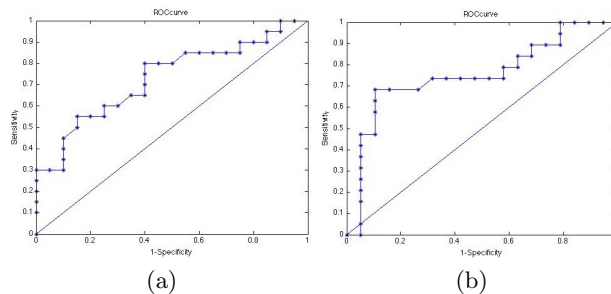

(a)   (b)

Fig. 3. ROC curves corresponding to: (a) system using manual external and internal segmentation done by the doctors and (b) the fully-automatic system.

[8]. Second row correspond to the "replica" of these results using the manual external and internal segmentation on the test set randomly defined by us. Finally, third row includes the results for the fully-automatic system, composed by the automatic external segmentation with CaudateCut and the automatic internal segmentation with linear SVM and DS. This fully-automatic system is giving results comparable with manual results, and can detect 68.42% of ADHD children correctly with only 11% of incorrect diagnostics on healthy subjects. In Figure 3, we show the ROC curve obtained based on the ratio value and corresponding to the system using manual external and internal segmentation done by the doctors in (a) and the fully-automatic system in (b).

Finally, we used a leave-one-out validation strategy on the set of 78 subjects to completely evaluate the proposed diagnostic test in the whole data set. In each test, we used ROC curve analysis to learn the OCOV as the optimal volume ratio threshold (specificity $\geq$ 85%). Table 2 (second row) contains the mean sensitivity, specificity and OCOV of the leave-one-out validation. This fully-automatic system shows acceptable results to assist the diagnostic of ADHD.

4   Conclusion

We presented a fully automatic strategy to assist in the diagnosis of ADHD in the pediatric population. Up to our knowledge, there not exists previous imaging test for ADHD diagnosis. Inspired in a previously presented manual study stating that the ratio between rCBV and bCBV was statistically different in ADHD and

control groups, we proposed an automatic approach consisting in the following steps: 1) external caudate segmentation using the recently proposed CaudateCut segmentation algorithm, 2) a novel internal caudate classification of head and body regions based on shape features and a machine learning approach, and 3) a ADHD diagnostic test. We performed separated validation process of steps 2) and 3) in real data, obtaining highly similar results to manual annotations in both cases.

Acknowledgements.

References

1. Carmona, S., Vilarroya, O., Bielsa, et. al.: Global and regional gray matter reductions in ADHD: A voxel-based morphometric study. Neuroscience Letters 389(2), 88–93 (2005)
2. Castellani, U., Mirtuono, P., Murino, V., Bellani, M., Rambaldelli, G., Tansella, M., Brambilla, P.: A new shape diffusion descriptor for brain classification. In: MICCAI (2). pp. 426–433 (2011)
3. Castellanos, F.X., Lee, P.P., Sharp, W., Jeffries, N.O., Greenstein, D.K., Clasen, L.S.e.a.: Developmental Trajectories of Brain Volume Abnormalities in Children and Adolescents With Attention-Deficit/Hyperactivity Disorder. The Journal of the American Medical Association 288(14), 1740–1748 (Oct 2002)
4. Gerig, G., Styner, M., Jones, D., Weinberger, D., Lieberman, J.: Shape Analysis of Brain Ventricles Using SPHARM. Mathematical Methods in Biomedical Image Analysis, IEEE Workshop on 0, 171–178 (Aug 2001), `http://dx.doi.org/10.1109/MMBIA.2001.991731`
5. Igual, L., Soliva, J.C., Hernandez-Vela, A., Escalera, S., Jimenez, X., Vilarroya, O., Radeva, P.: A fully-automatic caudate nucleus segmentation of brain MRI: Application in pediatric attention- deficit/hyperactivity disorder volumetric analysis. BioMedical Engineering Online 10(105)
6. Kolmogorov, V., Zabih, R.: What energy functions can be minimized via graph cuts. PAMI 26, 65–81 (2004)
7. Seidman, L.J., Valera, E.M., Makris, N.: Structural brain imaging of attention-deficit/hyperactivity disorder. Biological Psychiatry 57(11), 1263–1272 (2005)
8. Soliva, J., Fauquet, J., Bielsa, A., Rovira, M., Carmona, S., Ramos-Quiroga, J., Hilferty, J., Bulbena, A., Casas, M., Vilarroya, O.: Quantitative mr analysis of the caudate abnormalitites in pediatric adhd: Proposal for a diagnostic test. Psychiatric Research: Neuroimaging (2010)
9. Talairach, J., Tournoux, P.: Co-planar Stereotaxic Atlas of the Human Brain: 3-Dimensional Proportional System - an Approach to Cerebral Imaging. Thieme Medical Publishers (1988)
10. Trèmols, V., Bielsa, A., Soliva, J.C., Raheb, C., Carmona, S., Tomàs, J., Gispert, J., Rovira, M., Fauquet, J., Tobeña, A., Bulbena, A., Vilarroya, O.: Differential abnormalities of the head and body of the caudate nucleus in attention deficit-hyperactivity disorder. Psychiatric Research 163(3), 270–278 (2008)